



Projectile Break-up Effect on Fusion in $^{16}\text{O} + ^{156}\text{Gd}$ Reaction at Energy Range 4.3-6.3 MeV/A

Rahbar Ali^{a*}, D Singh^b, Harish Kumar^c, Suhail A Tali^c, Asif Khan^a, M Afzal Ansari^c,
R P Singh^d & S Muralithar^d

^aDepartment of Physics, G F (P G) College, Shahjahanpur 242 001, India

^bCentre for Applied Physics, Central University of Jharkhand, Ranchi 835 205, India

^cDepartment of Physics, Aligarh Muslim University, Aligarh 202 002, India

^dInter University Accelerator Centre, New Delhi 202 002, India

25 October 2020; accepted 4 December 2020

We discuss our present understanding of the incomplete fusion (ICF) reaction dynamics, the excitation function of six evaporation residues (ERs) have been measured in $^{16}\text{O} + ^{156}\text{Gd}$ reaction at projectile energy range, $E/A \sim 4.3-6.3$ MeV/Nucleon. Some of the ERs are produced directly & indirectly (*i.e.* through pre-cursor), the pre-cursor contributions have been separated out from the measured cumulative cross-section with the help of Cavinato *et al.*¹. After correcting the pre-cursor contribution, the independent yield has been compared with the statistical model code PACE-2², which describes the fusion reaction cross section. In order to optimize the parameter of the code PACE-2 that reproduces the cross section of all the complete fusion (CF) channels like xn and/or pxn-channels. Using the same set of input parameters, cross section of the ERs populated via incomplete fusion (ICF) channels have been measured. The enhancement in the measured cross section of the ERs populated via ICF channels over the PACE-2 prediction have been measured, which indicates the occurrence of the break-up of projectile ^{16}O into ($^{12}\text{C}+\alpha$) and/or ($^8\text{Be}+2\alpha$) leading to ICF reaction dynamics.

Keywords: Complete and Incomplete fusion reactions; Excitation function measurements; Mass-asymmetry; Projectile structure effect.

1 Introduction

In the last four decades, great efforts have been made in the study of fusion process in heavy ion induced reactions. It has been shown that at energies not too much above the Coulomb barrier, the fusion process was playing an important role in reaction cross section³⁻⁶. The widely used statistical model code PACE-2², describes the fusion cross section. While at higher energies, fusion process gives the way to incomplete fusion (ICF), where projectile fragmentation will takes place and decreasing the reaction cross section corresponding to the fusion. It has been experimentally established that complete fusion (CF) and incomplete fusion (ICF) is the dominating mode of reaction at energies above the coulomb barrier⁷⁻⁹. Fusion occurs, when interacting nuclei have sufficient kinetic energy to overcome the coulomb barrier and are subsequently trapped inside the potential pocket to form the composite nucleus, in which all the angular momentum of the system is

retained. On the other hand, if only part of the projectile, following break-up, fuses with the target nucleus, the process is called incomplete fusion (ICF). It is assumed that un-fused part does not interact with target nucleus and behaves as a spectator. In case of ICF, an incompletely fused composite system is formed, where partial linear momentum of the projectile is given to the target nucleus and relatively less nucleonic degrees of freedom are involved as compared to CF. This incompletely fused composite system having less charge and mass in-comparison to completely fused composite nucleus. However, first experimental evidence for ICF process was observed by Inamura *et al.*¹⁰. Subsequently, Glain *et al.*¹¹ provided the significant information of ICF reaction dynamics from the break-up of the projectile. Further, aremarkable and an impressive review of various utmost studies was also summarized by Parker *et al.*¹² and Gomes *et al.*¹³. These review clearly indicated that ICF of the projectile occurs at beam energies below 10 MeV/nucleon. Until now, there is no theoretical model available, which could reproduce

*Corresponding author (E-mail:rahbara@gmail.com)

the ICF data satisfactorily below 8 MeV/nucleon, hence experimental study of ICF is still an active area of research. Recent studies based on the EF measurements have shown that ICF also contributes significantly in the formation of ERs¹⁴⁻¹⁷. As a matter of fact, a large number of out-going reaction channels are opened in heavy ion induced reactions at moderate excitation energy and analysis of excitation functions (EFs) of the evaporation residues may provide significant information about the CF and ICF reactions. From the analysis of measured EFs, it has been observed that ICF process has a substantial contribution to the reaction cross-sections. In view of the literature, we have observed that ICF reaction studies are confined to medium mass target nuclei and very few studies are available with heavier targets ($A > 150$). In low and medium mass target nuclei, ICF cross-section is a small fraction of the total fusion cross section of the ERs. But, in heavier target nuclei, the α -particle (s) emission from the compound nucleus (CN) becomes less probable because of the high Coulomb barrier. As a result, ICF cross section associated with α -particle emission contributes the dominant component in the total fusion cross section. With this aim, an attempt has been made to study ICF reaction for $^{16}\text{O} + ^{156}\text{Gd}$ system at projectile energy in laboratory system ranging from 68 to 98 MeV. In the present measurement, six EFs of the ERs have been measured and compared with the statistical model code PACE-2. In these measurements, we have deduced the precursor contributions from the measured cumulative cross-section to get the independent cross-section of ERs. This paper is organized as follows. The experimental details are discussed in section-2. Measured EF data analysis with code PACE-2 and their interpretation are given in section 3. Finally, summary and conclusions of the present work are given in section 4. To the best of our knowledge, the present measurements for the given projectile-target system has been reported for the first time.

2 Essentials of Experimental Setup

The experiment discussed here for the measurement of EFs was performed at 15UD Pelletron of Inter University Accelerator Centre (IUAC), New Delhi. Beams of $^{16}\text{O}^{+7}$ ions with energy ~ 100 MeV from Pelletron focused on stack of the ^{156}Gd enriched targets (abundance $\sim 94.6\%$) of thickness lying ~ 1.2 - 2.5 $\text{mg}\cdot\text{cm}^{-2}$ which is placed at the center of the scattering chamber. In the present

measurement, EFs for $^{16}\text{O} + ^{156}\text{Gd}$ system were measured using recoil catcher activation technique followed by γ -ray spectrometry. The enriched targets ^{156}Gd (abundance $\approx 94.8\%$) of variable thickness lying between 1.2 - 2.2 $\text{mg}\cdot\text{cm}^{-2}$ were prepared by rolling machine at IUAC, New Delhi, India. While, Al-catcher cum energy degraders of thickness lying between ~ 1.2 - 2.5 $\text{mg}\cdot\text{cm}^{-2}$ were also prepared by rolling machine. The Al backings of ^{156}Gd samples served as energy degraders as well as catchers for recoiling residues that may be trapped into its thickness during the irradiation. The thickness of samples ^{156}Gd and Al degraders were determined by using microbalance as well as by the α -particle transmission method, based on the measurement of energy lost by 5.487 MeV α -particles obtained from ^{241}Am source, while traversing through the targets and energy degraders. The mean thickness of each target was measured by transmission of α -particles at different places of the targets to minimize the uncertainty in target thickness. Each target was cut into the pieces of 1.5×1.5 cm^2 and were pasted on Al holders having concentric holes of diameter 10 mm. The Al holders were used for rapid heat dissipation. In the present experiment, targets for irradiation were taken in the form of the stacks of these target interspersed with thin aluminum foils of desired thicknesses wherever needed. The aluminum backing of target material ^{156}Gd along with aluminum foils served both as energy degraders as well as catchers for recoiling residues that may be trapped into its thickness. Two stacks of ^{156}Gd targets (each containing 4 and 3 samples respectively) were irradiated separately at projectile energy 100 MeV and 95 MeV to encompass the energy range between 68 - 98 MeV. Keeping in view the half-lives of interest, stack-I was irradiated for about 2 hours with beam current ~ 14 nA and stack-II was irradiated for about 3 hours with beam current ~ 15 nA. Moreover, the stack of targets along with Al catcher foils were placed normal to the beam direction so that recoiling nuclei populated during the irradiation of the targets were trapped in the Al-catcher foils and hence there is no loss of activity from the sample and hence, gives rise to the better accuracy in the present measurements. As the incident beam passes through the stack, it loses its energy both in target material and Al-catcher foils. As such, successive targets of the stack get irradiated at different energies. The energies of ^{16}O -ion beam on the successive targets have been calculated using stopping power values obtained from code SRIM08¹⁸

based on energy-range formulations. In these calculations, energy straggling has not been taken into account due to its insignificant contribution. The beam flux was measured by the total charge collected at the Faraday cup, placed behind the target-catcher assembly. After the irradiation, stack of the targets along with Al degraders were taken out from the scattering chamber and induced activities produced in various targets along with Al degraders were recorded by pre-calibrated High Purity Germanium (HPGe) detector, which is coupled to PC based data acquisition system. The energy calibration of the detector was done by ^{152}Eu source of known strength. The resolutions of the HPGe detectors were found to be 2 keV at 1.33 MeV γ -rays of ^{60}Co , respectively. To record the induced activity in the irradiated samples, the distance between samples and detector was adjusted in such a way that dead time of the detector should be less than 10%. The γ -ray energy spectrum of the induced activity in the sample obtained from the interaction of ^{16}O with ^{156}Gd at projectile energy ~ 93 MeV is shown in Fig. 1. The identification of the reaction products populated via CF and/or ICF have been done by the characteristic γ -rays of the reaction products and also by following their half-lives. The measured half-lives of the residues were found to be in good agreement with literature values. The different peaks in γ -ray spectra have been assigned to the various radio-nuclides that may be populated via CF and/or ICF.

3 Analysis and Interpretation of Results

In the present work, the experimentally measured cross sections have been compared with the theoretical values calculated using different values of level density parameters 'K'. The PACE-2 calculations are carried out for ERs formed in CF reaction and the parameters of the code are optimized so as to reproduce the cross section of ERs produced exclusively through CF, *e.g.*, xn and pxn channels. Adopting the same set of optimized parameters, calculations have been performed consistently for all the expected ICF residues that are produced in the break-up of projectile into α -clusters. Any increase in the experimental cross section values over the PACE-2 prediction is taken as a signature of ICF. It may however important to note that ICF is not taken into account in PACE-2 calculations and hence enhancement, if any, in the measured EFs over PACE-2 predictions, for the residues that are populated in the break-up of projectile into α -cluster(s), may be attributed to the ICF process. The EFs of six radio-nuclides ^{168}Hf (4n), ^{166}Hf (6n), ^{167}Yb (α n), ^{164}Yb (α 4n), ^{166}Tm (α p4n) and ^{161}Er (2α 3n) have been measured in the interaction of ^{16}O with ^{156}Gd at ~ 68 -98 MeV beam energies. The reaction products ^{168}Hf and ^{166}Hf having half-lives 25.9 min and 6.8 min are populated via 4n and 6n emission channels from the composite system $^{172}\text{Hf}^*$ produced through CF of ^{16}O with ^{156}Gd . The measured EFs have been compared with statistical model code PACE-2 with

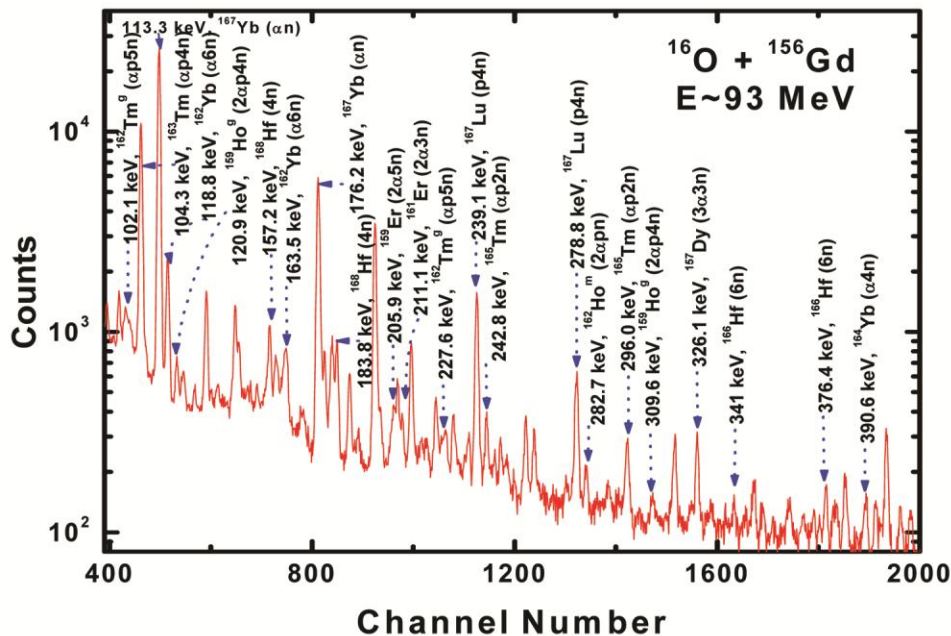
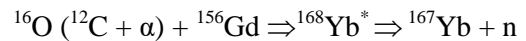
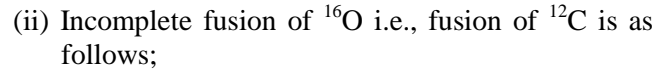
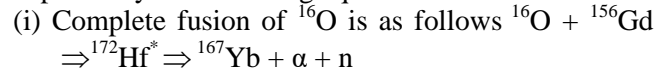


Fig. 1 — Typical γ -ray energy spectrum obtained after the irradiation of the ^{156}Gd target with ^{16}O -ion beam at energy ~ 93 MeV.

different values of level density parameter ($K = 8, 10, 12$) to match the experimental values and are displayed in Fig. 2. It has been observed from the Fig. 2 that the value of $K = 10$ reproduces the measured EF data well. Further, measured EFs for the residues populated in 1α -emission products, namely ^{167}Yb (αn), ^{164}Yb ($\alpha 4n$), ^{166}Tm (αpn) are shown in Fig. 3. As such negligible precursor contributions have been found in production of the residues ^{167}Yb (αn), ^{164}Yb ($\alpha 4n$), ^{166}Tm (αpn); hence measured cross sections are independent one. The measured cross sections are compared with PACE-2 predictions for the same value of $K=10$, used for the reproduction of CF channels. It can be seen from Fig. 3 that the measured cross sections are enhanced over the PACE-2 predictions. This indicates that the reaction products ^{167}Yb , ^{164}Yb and ^{166}Tm are populated via CF and/or ICF in the interaction of ^{16}O with ^{156}Gd . Residues produced via ICF of the projectile may be understood by the break-up of the projectile ^{16}O into the fragments ($^{12}\text{C} + ^4\text{He}$) in the target nuclear field;

one of the fragments ^{12}C fuses with ^{156}Gd , forming composite system $^{168}\text{Yb}^*$ which subsequently de-excite by the emission of $1n, 4n$, and $1p1n$ along with an α -particle as a spectator in the forward direction. In case of CF of ^{16}O with ^{156}Gd , the composite system $^{172}\text{Hf}^*$ is formed, which may de-excite by the evaporation of an α -particle along with $1n, 4n$ and $1p1n$ leaving behind residual nucleus ^{167}Yb , ^{164}Yb and ^{166}Tm respectively. As an example, the production of residue ^{167}Yb by CF and ICF processes may be depicted by the following equations:



(α -particle as spectator)

On the other hand, evaporation residue ^{161}Er ($2\alpha 3n$) having half-life 3.24 hrs are produced in 2α -emitting

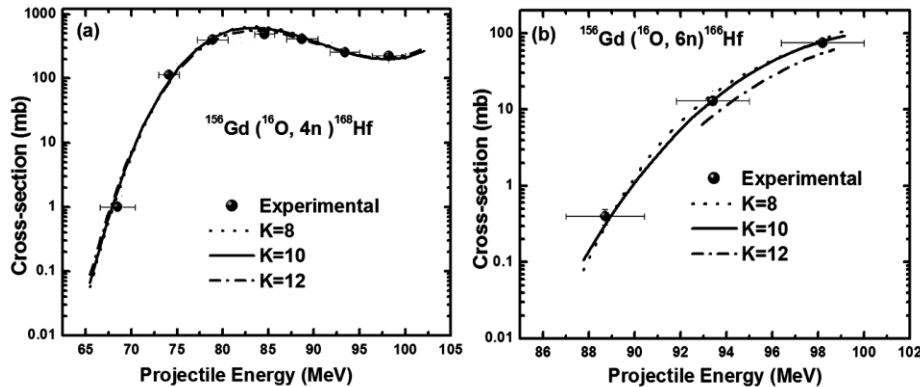


Fig. 2 — Excitation functions for evaporation residues ^{168}Hf and ^{166}Hf produced in $^{16}\text{O} + ^{156}\text{Gd}$ reaction. Solid circles represent the experimental data. Solid, dotted and dash-dotted lines correspond to theoretical predictions of the code PACE-2 for different values of K .

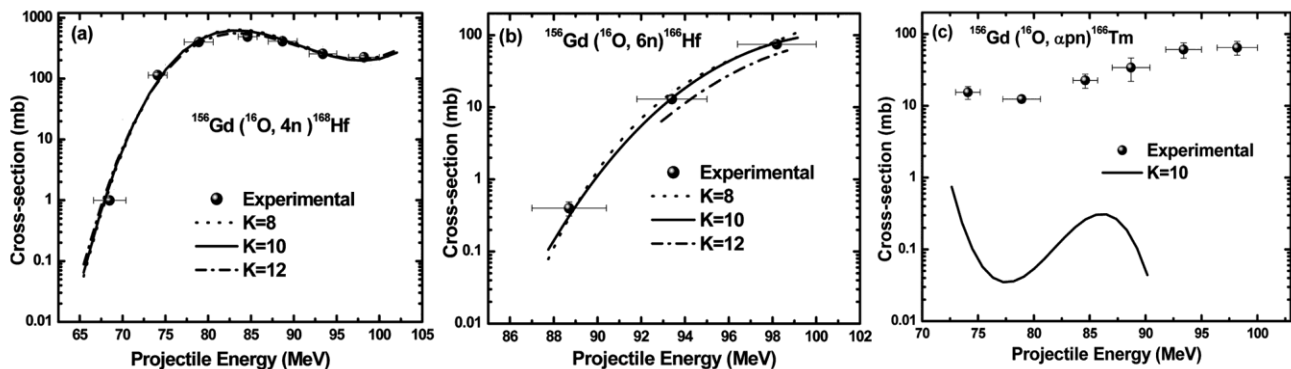


Fig. 3 — Excitation functions for ERs ^{167}Yb , ^{164}Yb & ^{166}Tm produced in $^{16}\text{O} + ^{156}\text{Gd}$ reaction. Solid circles represent the experimental data. Solid line corresponds to theoretical predictions of the code PACE-2 for $K=10$.

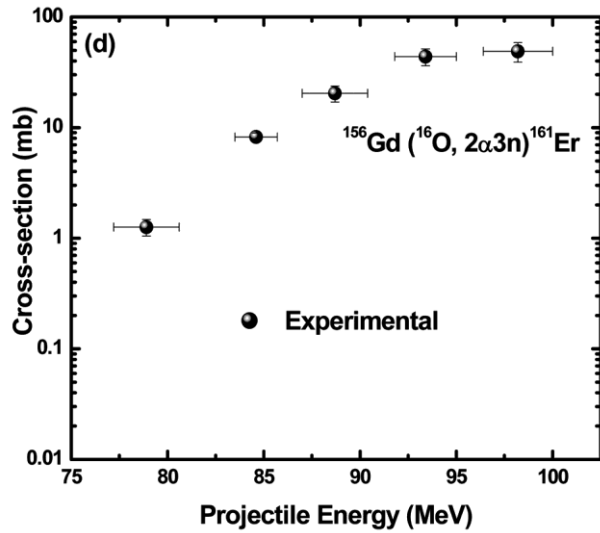


Fig. 4 — Excitation function for ER ^{161}Er produced in $^{16}\text{O} + ^{156}\text{Gd}$ reaction. Solid circles represent the experimental data. Solid line corresponds to theoretical predictions of the code PACE-2 for values of $K=10$.

channels and is shown in Fig. 4. As can be seen from Fig. 4, no theoretical predictions from PACE-2 are available. Hence, the residue ^{161}Er is solely produced via ICF of ^{16}O (*i.e.* fusion of fragment ^8Be with the target ^{156}Gd), forming composite system $^{164}\text{Er}^*$, which decays by emission of 3n along with 2α -particles as spectator which moves in forward direction. Since precursor contribution is small, so hollow and solid circles are just overlapping in excitation functions of these ERs.

4 Conclusions

Excitation functions of six evaporation residues populated through complete and/or incomplete fusion reaction have been measured in the $^{16}\text{O} + ^{156}\text{Gd}$ system in the projectile energy range ~ 4.3 -6.3 MeV/nucleon in laboratory frame. It has been observed that the evaporation residues populated through complete and/or incomplete fusion have negligible contribution from their pre-cursor decay of higher charge isobars during the decay curve analysis. The independent production cross-section and precursor decay contribution have been separated out from their measured cumulative cross-sections. The independent cross-section of the evaporation residues may be deduced by Cavinato *et al.*, formulism¹. The experimentally measured excitation functions have been compared with statistical model code PACE-2² based on compound nucleus theory. The experimentally measured EFs of the ERs after

correcting the pre-cursor contribution populated via 6n and p4n emission channels from the composite nucleus ^{172}Hf may be satisfactorily reproduced by the theoretically calculated EFs by code PACE-2, indicating their production through CF process only. A significant enhancement in the measured EFs over their theoretical predictions of PACE-2 for ERs populated through alpha particle(s) emitting channel has been found. This enhancement may be attributed to the occurrence of ICF involving the break-up of the projectile ^{16}O into $(^{12}\text{C}+\alpha)$ and/or $(^8\text{Be}+2\alpha)$ followed by fusion of one of the fragments with the target nucleus ^{156}Gd . Hence, it is inferred that incomplete fusion reaction plays an important role in the production of evaporation residues involving single or cluster of alpha particle emission at these projectile energies. The present findings of ERs populated through CF and/or ICF are consistent with our earlier measurements¹⁹ using particle- γ coincidence for same Z_p and Z_T at projectile energy 100 MeV.

Acknowledgements

Authors wish to thank Director, IUAC-New Delhi for providing me experimental facility to carry out research experiment. Special thanks are given to the members of the Pelletron group for providing the good quality beam of $^{16}\text{O}^{+7}$ and their co-operation during the course of the experiment.

References

- 1 Cavinato M, Fabrici E, Gadioli E, Gadioli E E, Vergani P, Crippa M, Colombo G, Redaelli I & Ripamonti M, *Phys Rev C*, 52 (1995) 2577.
- 2 Garvon A, *Phys Rev C*, 21 (1980) 230.
- 3 Singh D, Ansari M A, Ali R, Sathik N P M & Ismail M, *J Phys Soc Jpn*, 75 (2006) 104201.
- 4 Singh D, Ansari M A, Ali R, Sathik N P M & Ismail M, *Chin J Phys*, 46 (2008) 1.
- 5 Dasgupta M, Gomes P R S, Hinde D J, Moraes S B, Anjos R M, Berriman A C, Butt R D, Carlin N, Lubian J, Morton C R, Newton J O & Toledo A S de, *Phys Rev C*, 70 (2004) 026606.
- 6 Chakrabarty S, Tomar B S, Goswami A, Gubbi G K, Manohar S B, Sharma A, Kumar B B & Mukherjee S, *Nucl Phys A*, 678 (2000) 355.
- 7 Kumar H, Tali S A, Ansari M A, Singh D, Ali R, Kumar K, Sathik N P M, Ali A, Parashari S, Dubey R, Bala I, Kumar R, Singh R P & Muralithar S, *Eur Phys J A*, 54 (2018) 47.
- 8 Shuaib M, Sharma V R, Yadav A, Singh P P, Sharma M K, Singh D P, Kumar R, Singh R P, Muralithar S, Singh B P & Prasad R, *Phys Rev C*, 94 (2016) 014613.
- 9 Tali S A, Kumar H, Ansari M A, Ali A, Singh D, Ali R, Giri P K, Linda S B, Parashari S, Kumar R, Singh R P & Muralithar S, *Nucl Phys A*, 970 (2018) 208.

- 10 Inamura T, Ishihara M, Fukuda T, Shimoda T & Hiruta H, *Phys Lett B*, 68 (1977) 51.
- 11 Galin J, Gatty B, Guerreau D, Rousset C, Scholtthauer-Voos U C & Tarrago X, *Phys Rev C*, 9 (1974) 1126.
- 12 Parker D J, Hogson J J & Asher J, *Phys Rev C*, 39 (1989) 2256.
- 13 Gomes P R S, Padron I, Rodriguez M D, Marti G V, Anjos R M, Lubian J, Veiga R, Liguori N R, Crema E, Added N, Chamon L C, Fernandez N J O, Capurro O A, Pacheco A J, Testoni J E, Abriola D, Arazi A, Ramirez M & Hussein M S, *Phys Lett B*, 601 (2004) 20.
- 14 Tali S A, Kumar H, Ansari M A, Ali A, Singh D, Ali R, Giri P K, Linda S B, Kumar R, Parashari S, Singh R P & Muralithar S, *Indian J Pure Appl Phys*, 57 (2019) 544.
- 15 Tomar B S, Goswami A, Reddy A U R, Das S K, Burte P P, Manohar S B & Bency J, *Phys Rev C*, 49 (1994) 941.
- 16 Ali R, Singh D, Ansari M A, Rashid M H, Guin R & Das S K, *J Phys G Nucl Phys*, 37 (2010) 115101.
- 17 Singh D, Ali R, Ansari M A, Rashid M H, Guin R, Das S K, *Phys Rev C*, 83 (2011) 054604.
- 18 Ziegler J F, SRIM08, <http://www.srim.org/>, the Stopping Power and Range of Ions in Matter, 2008.
- 19 Ali R, Ansari M Afzal, Singh D, Kumar R, Singh D P, Sharma M K, Gupta U, Singh B P, Shidling P D, Negi D, Muralithar S, Singh R P & Bhowmik R K, *Nucl Phys A*, 968 (2017) 403.